Likelihood Function for QRM-MLD Suitable for Soft-Decision Turbo Decoding and Its Performance for OFCDM MIMO Multiplexing in Multipath Fading Channel

Kenichi Higuchi†, Hiroyuki Kawai†, Noriyuki Maeda†, Mamoru Sawahashi†, Takumi Itoh††, Yoshikazu Kakura††, Akihisa Ushirokawa††, and Hiroyuki Seki†††

†NTT DoCoMo, Inc.
3-5 Hikari-no-oka, Yokosuka-shi,
Kanagawa-ken, 239-8536 Japan
E-mail: higuchi@mlab.yrp.nttdocomo.co.jp

††NEC Corporation
1753 Shimonumabe, Nakahara-ku, Kawasaki-shi,
Kanagawa-ken, 211-8666 Japan

†††Fujitsu Laboratories Ltd.
5-5 Hikari-no-oka, Yokosuka-shi,
Kanagawa-ken, 239-0847 Japan

Abstract - This paper proposes likelihood function generation of complexity-reduced Maximum Likelihood Detection with QR Decomposition and M-algorithm (QRM-MLD) suitable for soft-decision Turbo decoding and investigates the throughput performance using QRM-MLD with the proposed likelihood function in multipath Rayleigh fading channels for Orthogonal Frequency and Code Division Multiplexing (OFCDM) with multiple-input multiple-output (MIMO) multiplexing. Simulation results show that by using the proposed likelihood function generation scheme for soft-decision Turbo decoding following QRM-MLD in 4-by-4 MIMO multiplexing, the required average received signal energy per bit-to-noise power spectrum density ratio (E_b/N_0) at the average block error rate (BLER) of 10^{-2} at a 1-Gbps data rate is significantly reduced compared to that using hard-decision decoding in OFCDM access with 16 QAM modulation, the coding rate of 8/9, and 8-code multiplexing with a spreading factor of 8 assuming a 100-MHz bandwidth. Furthermore, we show that by employing QRM-MLD associated with soft-decision Turbo decoding for 4-by-4 MIMO multiplexing, the throughput values of 500 Mbps and 1 Gbps are achieved at the average received E_b/N_0 of approximately 4.5 and 9.3 dB by QPSK with the coding rate of $R = 8/9$ and 16QAM with $R = 8/9$, respectively, for OFCDM access assuming a 100-MHz bandwidth in a twelve-path Rayleigh fading channel.

I. Introduction

For future mobile communication systems beyond the 3G system, it is considered that radio access networks (RANs) with a short delay (i.e., low latency) and with good affinity to IP-based core networks are desirable. In addition, a broadband approach shows promise in providing rich high-rate services at low cost via RANs. In such a broadband channel comprising many multipaths, members of our research group clarified that Orthogonal Frequency and Code Division Multiplexing (OFCDM), which is originally based on multi-carrier CDMA (MC-CDMA) [1]-[3], or orthogonal frequency division multiplexing (OFDM) exhibits better performance than conventional DS-CDMA based wireless access in the forward link [4] (note that we use the term OFCDM instead of MC-CDMA to distinguish it explicitly from the forward link access in the CDMA2000 system). This is because OFCDM and OFDM mitigate the degradation due to severe multipath interference in a broadband channel using many low symbol-rate sub-carriers, and make full use of the frequency diversity effect by using the spread and coded signals over parallel sub-carriers. As a result, OFCDM and OFDM are promising candidates for broadband wireless access in the forward link for the systems beyond IMT-2000. Members of our research group recently proposed OFCDM with variable spreading factor (VSF) packet wireless access (hereafter VSF-OFCDM) [5], [6], which changes the spreading factor, *SF*, of OFCDM in accordance with the cell structure and radio link conditions such as the delay spread, including the special no-spreading mode in the frequency domain. Through VSF-OFCDM, the seamless and flexible deployment of the same wireless access method both in multi-cell environments such as cellular systems and in isolated-cell environments such as hotspot areas or indoor offices is possible, while still achieving the maximum link capacity in the respective environments.

In local areas such as a very-small cell with high traffic density, hotspot area, or indoor environment, data rates even higher than that of cellular systems are needed with a large coverage area. In such local areas, since time dispersion, i.e., time delay of a path, is short in general owing to the short coverage area, utilization of multiple-input multiple-output (MIMO) multiplexing is promising [7], [8]. The signal transmission method called the Bell Laboratories layered space time (BLAST) that efficiently multiplexes a physical channel with the same radio resources, i.e., time, frequency and code, was proposed to take advantage of the features of the MIMO channel [7]. In the V-BLAST method [9], transmitted signals are separated by utilizing beam nulling and successive interference cancellers. Among decoding schemes, nevertheless, maximum likelihood detection (MLD) [10] can reduce the required signal energy per-bit-noise power spectrum density ratio (E_b/N_0) satisfying the required average bit error rate or block error rate (BLER) better than can V-BLAST or the Minimum Mean Squared Error (MMSE) methods. Thus, from the viewpoint of the achievable throughput increase, the MLD approach is the most promising. As is well known, however, the computational complexity in MLD is exponentially increased according to the increase in the modulation level in the data modulation scheme and the number of transmitter antenna branches. Accordingly, it is not practical to use conventional MLD without reducing the computational complexity (Full MLD, hereafter) because the computational complexity of MLD exceeds the level of an actual implementation. Regarding the actual implementation problem, a promising approach that applies QR decomposition associated with the M-algorithm to MLD (hereafter QRM-MLD) was proposed in [11], leading to a remarkable reduction in the computational complexity compared to that of Full MLD for OFDM MIMO multiplexing. Efficient channel coding (FEC: forward error correction) is essential to reducing the required received E_b/N_0 for wireless access. It is well known that soft-decision Turbo coding exhibits a large coding gain. In QRM-MLD, however, symbol replica candidates of the transmitted signals are successively reduced based on the M-algorithm after QR decomposition. Therefore, assuming soft-decision Turbo decoding, there is a problem in that the log likelihood ratio (LLR) of *a posteriori* probability (APP) for soft-decision Turbo decoding cannot be obtained when no surviving symbol replicas remain that contain either bit "1" or "-1" in QRM-MLD.

Therefore, this paper investigates the likelihood function of APP in QRM-MLD suitable for the subsequently employed soft-decision Turbo decoding for OFCDM MIMO Multiplexing. Furthermore, we present a QRM-MLD configuration based on

0-7803-8523-3/04/$20.00 ©2004 IEEE.

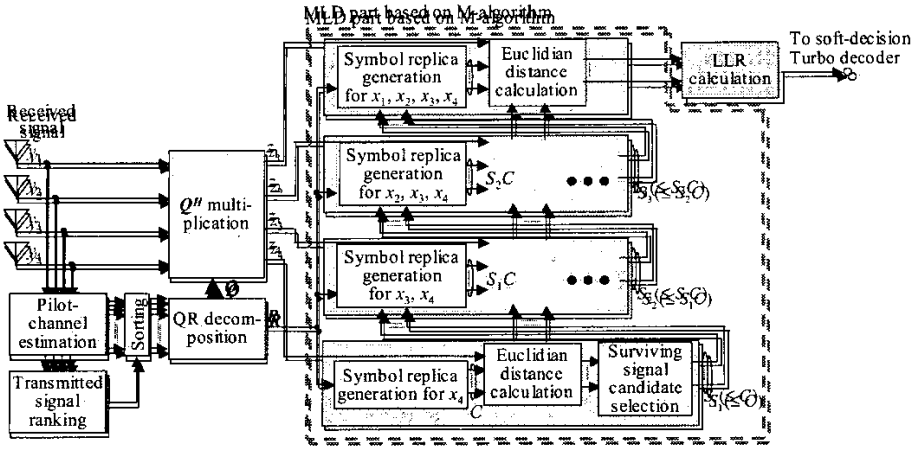

Figure 1. Configuration of pilot channel assisted QRM-MLD

channel estimation and the ranking of transmitted signals applying a time-multiplexed orthogonal pilot channel. Then, employing the configuration, the BLER and throughput performance using QRM-MLD followed by soft-decision Turbo decoding associated with the proposed likelihood function are investigated in multipath Rayleigh fading channels aiming at 1-Gbps throughput assuming a 100-MHz bandwidth. The rest of the paper is organized as follows. Section II first explains the operation of QRM-MLD for OFCDM. Next, Section III presents the proposed likelihood function suitable for soft-decision Turbo decoding. Then, after describing the simulation configuration in Section IV, the simulation results are presented in Section V showing 1-Gbps throughput assuming a 100-MHz bandwidth in a multipath fading channel.

II. QRM-MLD Configuration Using Pilot Channel-Assisted Channel Estimation and Ranking

Figure 1 illustrates the configuration of QRM-MLD using the pilot channel-assisted channel estimation and ranking. Figure 2 illustrates the packet frame format. One packet frame with the length of 0.5 msec consists of 48 coded data symbols and 4 time-multiplexed pilot symbols. The transmitted signal from the p-th ($1 \le p \le N_t$, N_t is the number of transmitter antenna branches) antenna branch is expressed as

$$s_p(t) = \sum_{k=1}^{N_{sub}} \sum_{i=1}^{N_{code}} d_{p,k,i}(nN_{frame}+b)c_{k,i}(nN_{frame}+b) \cdot e^{j2\pi k(t-T_g-(nN_{frame}+b-1)T_s)/T_d} p(t-(nN_{frame}+b-1)T_s), \quad (1)$$

where N_{sub} is the number of sub-carriers, N_{frame} is the number of OFCDM symbols in one frame, $d_{p,k,i}(nN_{frame}+b)$ is the b-th symbol ($1 \le b \le N_{frame}$) of the i-th ($1 \le i \le N_{code}$, N_{code} is the number of multicodes) code channel at the k-th ($1 \le k \le N_{sub}$) sub-carrier in the n-th (n: integer) packet frame from the p-th transmitter branch, and $c_{k,i}(nN_{frame}+b)$ denotes the spreading code sequence. Furthermore, T_s, T_d, and T_g are the OFCDM symbol duration, effective data symbol duration, and guard interval length, respectively ($T_s = T_g + T_d$). Term $p(t)$ is the pulse function defined within the duration of $[0, T_s)$ and $d_{p,k,i}(nN_{frame}+b)$ is given as

$$d_{p,k,i}(nN_{frame}+b) = \begin{cases} d_{p,pilot}(1), & \text{for } b=1 \\ d_{p,k,i}(n, \lfloor (b-2)/SF \rfloor), & \text{for } 2 \le b \le N_{frame}/2-1 \\ d_{p,pilot}(2), d_{pilot}(3), & \text{for } b = N_{frame}/2, N_{frame}/2+1 \\ d_{p,k,i}(n, \lfloor (b-4)/SF \rfloor), & \text{for } N_{frame}/2+2 \le b \le N_{frame}-1 \\ d_{p,pilot}(4), & \text{for } b = N_{frame} \end{cases}, \quad (2)$$

$0 \le l < L$

where $d_{p,pilot}(b)$ is an orthogonal pilot symbol sequence and SF denotes the spreading factor in the time domain (note that we use time domain spreading in the paper). The received signal at the q-th branch ($1 \le q \le N_r$, N_r is the number of received antenna branches), $y_q(t)$, is represented as

$$y_q(t) = \sum_{p=1}^{N_t} \sum_{l=1}^{L} f_{p,q,l}(t) s_p(t-\tau_l) + n_q(t), \quad (3)$$

where $f_{p,q,l}(t)$ and τ_l are the complex channel gain of the l-th path ( ) between the p-th transmitter branch and the q-th receiver branch and the time delay of the l-th path, respectively, and $n_q(t)$ is additive Gaussian noise. The OFCDM signal after FFT processing at the k-th sub-carrier is expressed as

$$y_{q,k}(nN_{frame}+b) = \sum_{p=1}^{N_t} \xi_{p,q,k}(n) \sum_{i=1}^{N_{code}} d_{p,k,i}(nN_{frame}+b) \cdot c_{k,i}(nN_{frame}+b) + n_{q,k}(nN_{frame}+b), \quad (4)$$

where $\xi_{p,q,k}(n)$ is the complex channel gain at the k-th sub-carrier and we assume it is constant over one packet frame for the sake of simplicity. The j-th data symbol after despreading, $\hat{d}_{q,k,i}(n,j)$, is given as

$$\hat{d}_{q,k,i}(n,j) = \sum_{b=1}^{SF} y_{q,k}(nN_{frame}+b+jSF) c_{k,i}^*(nN_{frame}+b+jSF) = \sum_{p=1}^{N_t} \xi_{p,q,k}(n) d_{p,k,i}(n,j) + w_{q,k,i}(n,j). \quad (5)$$

The channel gain at the k-th sub-carrier, $\xi_{p,q,k}(n)$, is esti

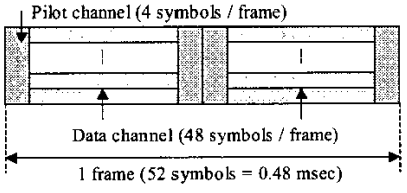

Figure 2. Packet frame format

mated by a two-dimensional multi-slot and sub-carrier-averaging (MSCA) channel estimation filter [12] using the orthogonal pilot channel as indicated below. We first derive the channel estimate of the target time slot and sub-carrier by coherently averaging four pilot symbols belonging to the frame as

$$\hat{\xi}_{p,q,k}(n)=\frac{1}{4}(y_{q,k}(nN_{frame}+1)d^{*}_{p,pilot}(1)c^{*}_{k,1}(nN_{frame}+1) + \sum_{b=1}^{2}\left(\begin{array}{l} y_{q,k}((n+1/2)N_{frame}-1+b) \\ \cdot d^{*}_{p,pilot}(b+1)c^{*}_{k,1}((n+1/2)N_{frame}-1+b)\end{array}\right) + y_{q,k}((n+1)N_{frame})d^{*}_{p,pilot}(4)c^{*}_{k,1}((n+1)N_{frame})) \quad (6)$$

The channel estimate of the n-th frame at the k-th sub-carrier, $\hat{\xi}_{p,q,k}(n)$, is further weighted and coherently combined with appropriate weights over $(2N_{Freq}+1)$ sub-carriers and $(2N_{Time}+1)$ frames with the k-th sub-carrier and the n-th slot as the center, respectively, as shown below.

$$\tilde{\xi}_{p,q,k}(n)= \frac{1}{\sum_{k'=-N_{Freq}}^{N_{Freq}}\sum_{n'=-N_{Time}}^{N_{Time}}\alpha_{Freq,k'}\alpha_{Time,n'}}\sum_{k'=-N_{Freq}}^{N_{Freq}}\sum_{n'=-N_{Time}}^{N_{Time}}\alpha_{Freq,k'}\alpha_{Time,n'}\hat{\xi}_{p,q,k+k'}(n+n') \quad (7)$$

where $\alpha_{Freq,k'}$ and $\alpha_{Time,n'}$ are the real-valued weighting factor for the $(k+k')$-th sub-carrier and the $(n+n')$-th slot. In this paper, we assume that $N_{Freq}=N_{Time}=1$. Furthermore, we set $\alpha_{Freq,k'}$ and $\alpha_{Time,n'}$ to $\alpha_{Freq,0}=1.0, \alpha_{Freq,\pm1}=0.2$ and $\alpha_{Time,0}, \alpha_{Time,\pm1}=1.0$ [12]. We estimate the received signal-to-interference plus noise power ratio (SINR) of each packet frame from the channel estimate in Eq. (7) and its variance using the pilot symbols within the frame. Thus, the transmitted signals are ranked according to the received SINR for every packet frame. In this way, accurate ranking of the transmitted signals is possible based on the received SINR utilizing all pilot symbols within a frame in our scheme.

Let $rank_k(p)$ be the transmitter branch index ranked at the p-th order at the k-th sub-carrier. Then, the estimate of the channel matrix for k-th sub-carrier after ranking is expressed as

$$\hat{\mathbf{H}}_k(n)=\begin{bmatrix} \hat{\xi}_{rank_k(N_t),1,k}(n) & \hat{\xi}_{rank_k(N_t-1),1,k}(n) & \cdots & \hat{\xi}_{rank_k(1),1,k}(n) \\ \hat{\xi}_{rank_k(N_t),2,k}(n) & \hat{\xi}_{rank_k(N_t-1),2,k}(n) & \cdots & \hat{\xi}_{rank_k(1),2,k}(n) \\ \vdots & & & \\ \hat{\xi}_{rank_k(N_t),N_r,k}(n) & \hat{\xi}_{rank_k(N_t-1),N_r,k}(n) & \cdots & \hat{\xi}_{rank_k(1),N_r,k}(n) \end{bmatrix} \quad (8)$$

Let $\mathbf{Q}_k(n)$ be the unitary matrix with the size of N_r x N_t. By performing QR decomposition for the estimate of the channel matrix as $\hat{\mathbf{H}}_k(n)=\mathbf{Q}_k(n)\mathbf{R}_k(n)$, the obtained matrix, $\mathbf{R}_k(n)$, becomes an upper triangular matrix with the size of N_t x N_t.

$$\mathbf{R}_k(n)=\mathbf{Q}_k(n)^{\mathrm{H}}\hat{\mathbf{H}}_k(n) = \begin{bmatrix} r_{1,1,k}(n) & r_{1,2,k}(n) & \cdots & r_{1,N_t,k}(n) \\ 0 & r_{2,2,k}(n) & \cdots & r_{2,N_t,k}(n) \\ \vdots & & & \\ 0 & \cdots & r_{N_t-1,N_t-1,k}(n) & r_{N_t-1,N_t,k}(n) \\ 0 & \cdots & 0 & r_{N_t,N_t,k}(n) \end{bmatrix} \quad (9)$$

By multiplying $\mathbf{Q}_k(n)^{\mathrm{H}}$ with the despread signal in vector notation of the i-th code channel at the k-th sub-carrier, $\mathbf{Y}_{k,i}(n,j)$, then the received signal in vector notation after nulling (i.e., orthogonalization), $\mathbf{Z}_{k,i}(n,j)$, is generated as

$$\mathbf{Z}_{k,i}(n,j)=\begin{bmatrix} z_{N_t,k,i}(n,j) \\ z_{N_t-1,k,i}(n,j) \\ \vdots \\ z_{1,k,i}(n,j) \end{bmatrix}=\mathbf{Q}_k(n)^{\mathrm{H}}\mathbf{Y}_{k,i}(n,j)=\mathbf{Q}_k(n)^{\mathrm{H}}\begin{bmatrix} \hat{d}_{1,k,i}(n,j) \\ \hat{d}_{2,k,i}(n,j) \\ \vdots \\ \hat{d}_{N_t,k,i}(n,j) \end{bmatrix} = \mathbf{R}_k(n)\begin{bmatrix} d_{rank_k(N_t),k,i}(n,j) \\ d_{rank_k(N_t-1),k,i}(n,j) \\ \vdots \\ d_{rank_k(1),k,i}(n,j) \end{bmatrix}+\begin{bmatrix} w'_{1,k,i}(n,j) \\ w'_{2,k,i}(n,j) \\ \vdots \\ w'_{N_t,k,i}(n,j) \end{bmatrix} \quad (10)$$

Next, we describe the operation of the M-algorithm. In QRM-MLD comprising stages corresponding to the number of transmitter branches, N_t, the symbol replica candidates with low reliability are successively discarded stage-by-stage using $\mathbf{Z}_{k,i}(n,j)$ and $\mathbf{R}_k(n)$ based on the M-algorithm. In the subsequent explanations, we omit the notations of n, k, i, and j; furthermore, we denote $rank_k(p)$ as p, for the sake of simplicity.

In the first stage ($m=1$), all symbol replica candidates c_x ($1 \le x \le C$, C denotes the number of constellations of each symbol) of the first transmitted signal are generated and the metric based on the squared Euclidian distance, $e_{m=1,1,x}$, between z_1 and symbol replica candidate c_x is calculated as

$$e_{1,1,x}=|z_1-r_{N_t,N_t}c_x|^2. \quad (11)$$

By comparing the squared Euclidian distances for all symbol replica candidates, S_1 ($S_1 \le C$) symbol-replica candidates are selected as $c_{m=1,1,p=1}$, ..., $c_{1,S_1,1}$ from the one with the smallest branch metric as the surviving symbol replica candidates, and preserving their metrics as $E_{m=1,1}$, ..., E_{1,S_1}. Since transmitted signals from other branches are not included in z_1, the surviving symbol candidates for the first branch are accurately selected.

In the second stage, for all the combinations ($S_1 C$) of S_1 surviving symbol replica candidates, $c_{1,1,1}$, ..., $c_{1,S_1,1}$, from the first branch and all symbol replica candidates, c_x, from the second branch, the accumulated branch metrics are updated from the branch metrics of the surviving symbols at the first stage and from the squared Euclidian distance between z_2 and all symbol replica candidates as

$$e_{2,y,x}=|z_2-(r_{N_t-1,N_t}c_{1,y,1}+r_{N_t-1,N_t-1}c_x)|^2+E_{1,y}. \quad (12)$$

Similar to the first stage, S_2 ($S_2 \le S_1 C$) symbol-replica candidates for the first and second branches, $\mathbf{c}_{m=2,1}=[c_{m=2,1,p=2}, c_{2,1,1}]^{\mathrm{T}}$, ..., $\mathbf{c}_{2,S_2}=[c_{2,S_2,2}, c_{2,S_2,1}]^{\mathrm{T}}$, are selected from the one with the smallest accumulated branch metric as the surviving symbol replica candidates, along with their accumulated branch metrics as $E_{2,1}$, ..., E_{2,S_2}. The process is repeated up to the last stage.

Finally, the LLR of the APP for each bit, $\hat{\Lambda}_{p,b}$, is calculated for the subsequently employed soft-decision Turbo decoding from theaccumulated branch metrics of the surviving symbol candidates at the last stage as

$$\hat{\Lambda}_{p,b}=\left(\sqrt{e_{\min,p,b,-1}}-\sqrt{e_{\min,p,b,1}}\right), \quad (13)$$

where $e_{\min,p,b,v}$ is the minimum squared Euclidian distance among the surviving symbols representing bit "v" for the b-th bit from the p-th transmitter antenna branch.

III. Likelihood Function of APP Suitable for Soft-Decision Turbo Decoding in QRM-MLD

To perform soft-decision channel decoding, the squared Euclidian distance representing both "1" and "-1" is needed

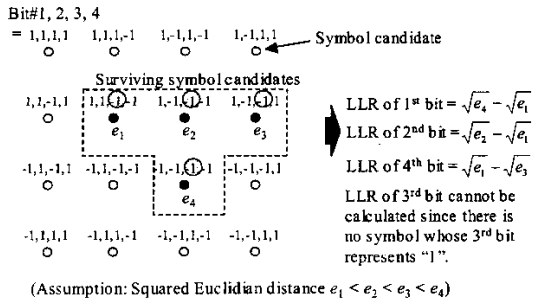

Figure 3. LLR calculation using surviving symbol candidates

for each bit in the remaining symbol replica candidates to calculate the $\hat{\Lambda}_{p,b}$ value. As described previously, a situation in which no surviving symbol candidates representing either bit "1" or "-1" remain occurs in QRM-MLD since symbol replica candidates with low reliability are discarded based on the M-algorithm as shown in Fig. 3 (it should be noted that the ratio of surviving symbol replicas containing only either bit "1" or "-1" is large such as approximately 20% assuming 4-by-4 MIMO multiplexing with 16QAM data modulation). Therefore, assuming soft-decision Turbo decoding, there is a problem such that the LLR of the APP for soft-decision Turbo decoding cannot be obtained when no surviving symbol candidates containing either bit "1" or "-1" remain at the last stage. Thus, we propose likelihood function generation that is suitable for the subsequent soft-decision Turbo decoding and the use of the Euclidian distance as a branch metric (i.e., reliability information).

3.1. Likelihood Function Generation

For the above-mentioned situation in QRM-MLD, although hard-decision Turbo decoding can be considered by setting an extremely large likelihood function for a non-existing bit, the achievable performance using hard-decision Turbo decoding will be significantly degraded compared to that using the soft-decision approach. Figure 4 shows the proposed likelihood function generation for bits when surviving symbol replica candidates do not remain to the last stage in QRM-MLD. In the proposed scheme, the likelihood function is generated in the following process.

(a) The minimum squared Euclidian distance of each bit is derived for the surviving symbol candidates.
(b) A larger minimum squared Euclidian distance is selected between squared Euclidian distance results in (a), in which the minimum squared Euclidian distance exists for both bits "1" and "-1".
(c) The minimum squared Euclidian distance selected in (b) is averaged among the bits, in which the minimum squared Euclidian distance exists for both bits "1" and "-1".
(d) The average minimum squared Euclidian distance over the remaining bits is further averaged over multiple symbols and then, multiplied by a factor of "X". We set X = 1.5 after near optimization based on simulations in the paper.

Table 1. Simulation Parameters.

Number of sub-carriers	768 (131.836 kHz sub-carrier spacing)
Number of IFFT/FFT points	1024
Spreading factor, *SF*	$SF_{Time} \times SF_{Freq} = 8 \times 1$
Number of multicodes	8
Data modulation / Spreading	QPSK, 16QAM / QPSK
OFCDM symbol duration (Effective data + Guard interval)	9.259 μsec (7.585 + 1.674 μsec)
Frame length	52 OFCDM symbols
Channel coding / Decoding	Turbo coding (R = 3/4, 8/9, K =4) / Max-Log-MAP decoding (Iterations = 8)
Symbol timing detection	Ideal
Channel estimation	Pilot symbol assisted channel estimation
Signal detection	(1) Full MLD (2) QRM-MLD (16QAM: $\{S_1, S_2, S_3\}$ = {16, 16, 16}, QPSK: $\{S_1, S_2, S_3\}$ = {4, 16, 16})
Transmit signal ranking for QRM-MLD	SINR-based ranking (every frame)

3.2. Application of Euclidian Distance as Branch Metric

In general, the squared Euclidian distance is used for calculating the LLR. In QRM-MLD, however, the Euclidian distance (i.e., the square root of the squared value) may be near optimum rather than the squared Euclidian distance in QRL-MLD because estimation errors in the likelihood function of bits, which do not remain among the surviving symbol candidates at the last stage, can be mitigated. Therefore, we propose using the Euclidian distance instead of the squared Euclidian distance and investigate the effect of the likelihood function employing the root of the squared value for the Euclidian distance.

IV. Simulation Configuration

Table 1 gives the parameters assumed in the subsequent simulation evaluations. We assume a 101.5-MHz bandwidth. Furthermore, we assume four transmitter/receiver antenna branches, i.e., 4-by-4 MIMO multiplexing.

At the transmitter, binary information data bits are first serial-to-parallel-converted into four data streams and are segmented into blocks containing a selected number of bits per packet frame according to the employed modulation and coding scheme (MCS). The information data sequence is encoded by Turbo coding with the original coding rate $R_{org} = 1/3$ and the constraint length of $K = 4$ bits, and then punctured according to the coding rate of $R = 3/4$ or 8/9. The resultant encoded sequence stream is data-modulated with QPSK or 16QAM. After serial-to-parallel conversion into 768 streams corresponding to the number of sub-carriers, the symbol sequence is interleaved over all the sub-carriers. The parallel symbol is spread over $SF_{Time} = 8$ symbols in the time domain by the combination of a short channelization code and a long scrambling code. By assigning different short channelization codes, the $C_{max} = 8$ code channels are code-multiplexed. Furthermore, the four orthogonal pilot symbols are time-multiplexed to spread coded data symbols. The spread data symbol sequence is converted into OFCDM signals with $N_{sub} = 768$ sub-carriers (= 1024-sample duration = 7.585 μsec) using the inverse fast Fourier transform (IFFT). In order to avoid inter-symbol interference caused by multipath propagation, a guard interval (= 226-sample duration = 1.674

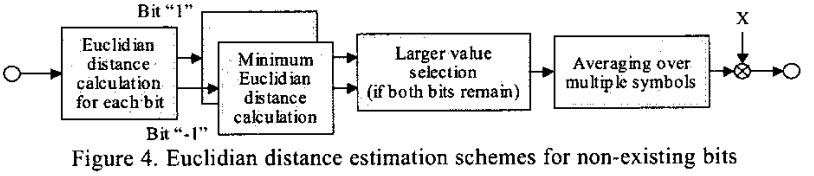

Figure 4. Euclidian distance estimation schemes for non-existing bits

μsec) is inserted between the OFCDM symbols. The resultant frame consists of 48 OFCDM data symbols and four pilot symbols (i.e., N_{frame} = 52). Transmission power ratio of pilot channel to one-code data channel is set to 9 dB.

At the receiver, we assume ideal OFCDM timing (i.e., FFT window timing) detection. After the guard interval is removed, the OFCDM signal is de-multiplexed into each sub-carrier component by the 1024-point FFT. The channel gain in each sub-carrier is estimated using the pilot channel. The transmitted data sequences from four antenna branches are ranked at each sub-carrier according to the SINR over one packet frame measured by pilot channels in descending order from the largest SINR branch. In the subsequent QRM-MLD, the number of surviving symbol-replica candidates in the first, second, and third stages in QRM-MLD is set to $S_1 = S_2 = S_3 = 16$ for 16QAM, respectively. Finally, output symbol streams of QRM-MLD are parallel-to-serial-converted and soft-decision Turbo decoded by Max-Log-MAP decoding with eight iterations to recover the transmitted binary data.

We evaluated the performance using an exponential decay model with an L-path Rayleigh fading profile with the fading maximum Doppler frequency of f_D = 20 Hz (i.e., corresponding to the average speed of 5 km/h assuming a 5-GHz carrier frequency), in which the average signal power of each path is reduced by 12/L dB in descending order starting from the first path. The r.m.s. delay spread, σ, is varied from approximately 0.09 to 0.51 μsec as a parameter by changing the time delay among paths. The fading correlation between two contiguous antenna branches, ρ, is also a parameter (the same value is assumed for the transmitter and receiver branches).

V. Simulation Results

5.1. Likelihood Function Suitable for Soft-decision Turbo Decoding

The average BLER performance using the proposed likelihood function described in Section III for QRM-MLD associated with soft-decision decoding is plotted in Fig. 5 as a function of the average received E_b/N_0 per receiver antenna branch. We assume 16QAM modulation and R = 3/4 and 8/9 with L = 12, σ = 0.26 μsec, and ρ = 0. In the evaluations in the paper, the estimated likelihood function for non-existing bit at each symbol is averaged in the code domain, time domains over one frame length and frequency domain over all the sub-carriers, respectively, to reduce the influence of background noise. The BLER performance using hard-decision Turbo decoding and that assuming LLR of zero when the bit remains only either bit "1" or "-1" (corresponding to puncturing) are also given in the figure. Figure 5 clearly shows that the BLER performance for soft-decision Turbo decoding using the proposed likelihood function for symbols without bit "1" or "-1" is significantly improved compared to that for hard-decision Turbo decoding following QRM-MLD. More specifically, the required average received E_b/N_0 at the average BLER of 10^{-2} employing the proposed method is reduced by approximately 4.2 and 2.0 dB compared to that with hard-decision decoding for R = 3/4 and 8/9, respectively. We find that the BLER performance using equivalent puncturing for the symbols without bit "1" or "-1" is significantly deteriorated.

5.2. Application of Euclidian Distance as Branch Metric

A comparison of the average BLER performance using the squared Euclidian distance and the Euclidian distance (i.e. the square root of the squared value) as the LLR in QRM-MLD is plotted in Fig. 6 as a function of the average received E_b/N_0 per receiver antenna branch. The other simulation conditions are identical to those in Fig. 5. The BLER performance for Full MLD is also given for comparison. As shown in Fig. 6, the average BLER performance using the LLR based on the Euclidian distance is significantly improved compared to that with the

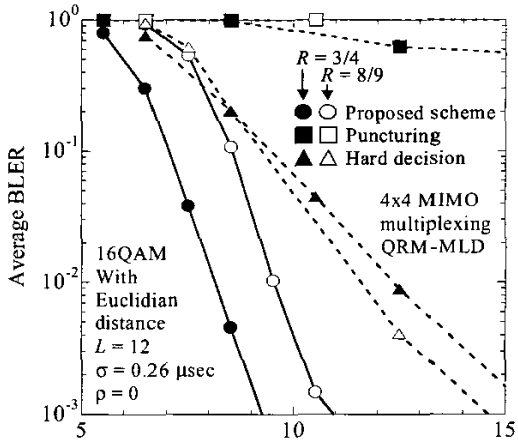

Figure 5. Comparison of Euclidian distance estimation schemes for non-existing bits

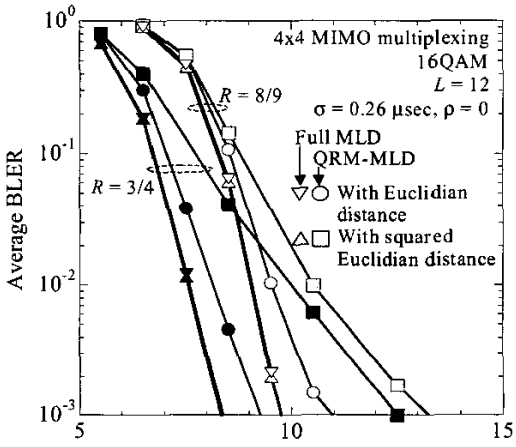

Figure 6. Comparison of LLR calculation schemes

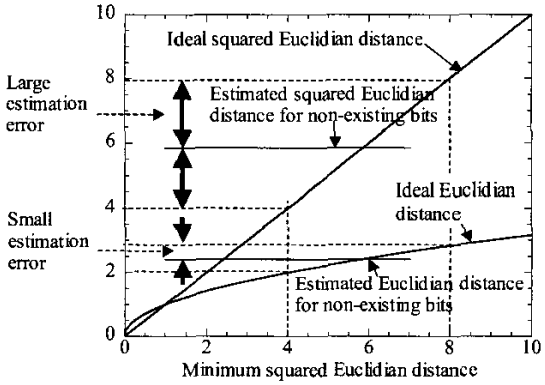

Figure 7. Squared Euclidian distance-based LLR calculation and Euclidian distance-based LLR calculation

squared Euclidian distance, although no difference is seen for the Full MLD. This is because the Euclidian distance can reduce the fluctuation in the signal level compared to that for the squared Euclidian distance as shown in Fig. 7, leading to a decrease in the error in the generated LLR for the bits when the surviving symbol does not exist at the last stage in QRM-MLD. Therefore, we conclude that the Euclidian distance should be used in QRM-MLD. We also find that the loss in the required average received E_b/N_0 of QRM-MLD from the Full MLD is only approximately 0.5 dB at the average BLER of 10^{-2}.

5.3. BLER and Throughput Performance Using QRM-MLD with Proposed Likelihood Function

Following the results in Sections 5.1 and 5.2, we investigate the average BLER and throughput performance using QRM-MLD associated with soft-decision Turbo decoding employing the proposed likelihood function generation based on the Euclidian distance.

(a) BLER for number of paths

The average received E_b/N_0 at the average BLER of 10^{-2} is plotted in Fig. 8 as a function of the number of paths, L, assuming $\sigma = 0.26$ μsec and $\rho = 0$. MCSs of 16QAM modulation with R = 3/4 and 8/9 are used (corresponding maximum data rates are 884 Mbps and 1.048 Gbps, respectively assuming a 100-MHz bandwidth). The performance using the Full MLD is also given in the figure for comparison. Figure 8 shows that according to the increase in the L value, the required average received E_b/N_0 is reduced due to the increasing frequency diversity effect. Even for the $L = 1$ case, by employing QRM-MLD, the average BLER of 10^{-2} is achieved at the average received E_b/N_0 of approximately 12.0 dB with $R = 8/9$. Moreover, we find that the loss in the required average received E_b/N_0 using the QRM-MLD from that with the Full MLD is suppressed within approximately 0.8 dB irrespective of the L value.

(b) BLER for r.m.s. delay spread

The required average received E_b/N_0 using QRM-MLD and the Full MLD is plotted in Fig. 9 as a function of σ with the same MCSs as in Fig. 8. The number of paths is set to $L = 12$, and the time delay between two consecutive paths is increased according to the increase in σ. Figure 9 shows that when σ is less than approximately 0.43 μsec (the corresponding maximum path delay is 1.63 μsec), the loss in the required average received E_b/N_0 with QRM-MLD from that with the Full MLD is within approximately 0.8 dB. When σ further increases, the required average received E_b/N_0 is increased due to channel estimation error. However, the average BLER of 10^{-2} using QRM-MLD is achieved at the average received E_b/N_0 of approximately 10.8 dB for $\sigma = 0.43$ μsec with the MCS of 16QAM modulation and $R = 8/9$.

(c) BLER for fading correlation between antenna branches

Figure 10 plots the average received E_b/N_0 at the average BLER of 10^{-2} using QRM-MLD and the Full MLD as a function of the fading correlation between the transmitter/receiver antenna branches, ρ, for $L = 12$ and $\sigma = 0.26$ μsec. The same MCSs as in Fig. 8 are assumed. We find that the loss in the required average received E_b/N_0 with QRM-MLD from that with the Full MLD is within approximately 1.5 dB when ρ is less than approximately 0.6. For instance, the required average BLER of 10^{-2} at the data rate of 1 Gbps is achieved at the average received E_b/N_0 of approximately 15.5 dB using the MCS of 16QAM and R = 8/9 even for $\rho = 0.6$.

(d) Throughput performance

Finally, the throughput of QRM-MLD and the Full MLD associated with soft-decision Turbo decoding is plotted in Fig. 11 as a function of the average received E_b/N_0. The data modulations are QPSK and 16QAM, and the channel coding

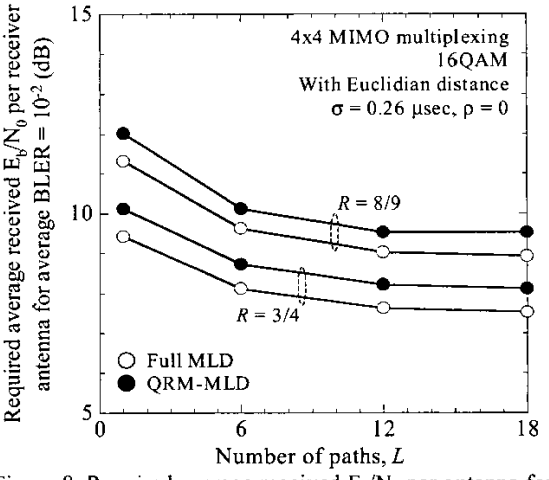

Figure 8. Required average received E_b/N_0 per antenna for average BLER = 10^{-2} as a function of L

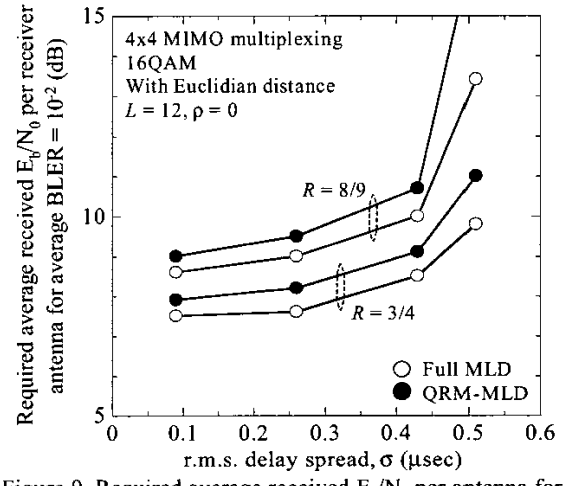

Figure 9. Required average received E_b/N_0 per antenna for average BLER = 10^{-2} as a function of σ

rates are R = 3/4 and 8/9. The maximum data rates for QPSK with R = 3/4 and 8/9 are approximately 441 and 523 Mbps, respectively. Throughput η (bit per second) is defined as

$$\eta = R_b \times \frac{N_{suc}}{N_{trans}}, \tag{14}$$

where R_b is the total information bit rate, and N_{trans} and N_{suc} are the total number of transmitted and correctly received packets, respectively. It is assumed that $L = 12$, $\sigma = 0.26$ μsec, and $\rho = 0$. The figure clearly shows that the throughput values of 400, 500, 850, and 1000 Mbps are achieved at the average received E_b/N_0 of approximately 2.5, 4.5, 7.5, and 9.3 dB by QPSK with R = 3/4, QPSK with 8/9, 16QAM with R = 3/4, and 16QAM with 8/9, respectively. Thus, we conclude that the QRM-MLD associated with soft-decision Turbo coding exploiting the proposed likelihood function when no surviving symbol replicas remain that contain either bit "1" or "-1" with the use of Euclidian distance as branch metric is effective in achieving very high frequency efficiency for OFCDM access even in a severe multipath fading channel.

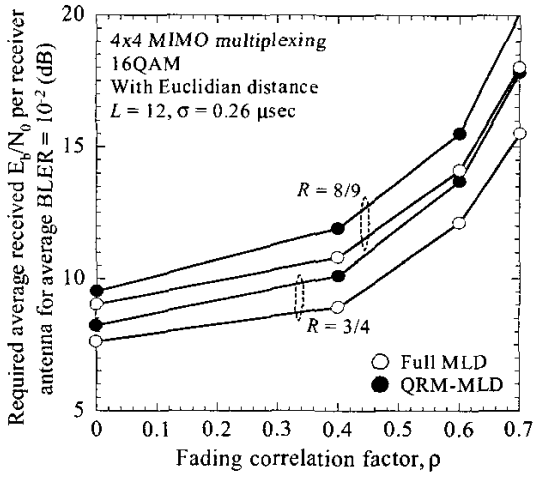

Figure 10. Required average received E_b/N_0 per antenna for average BLER = 10^{-2} as a function of ρ

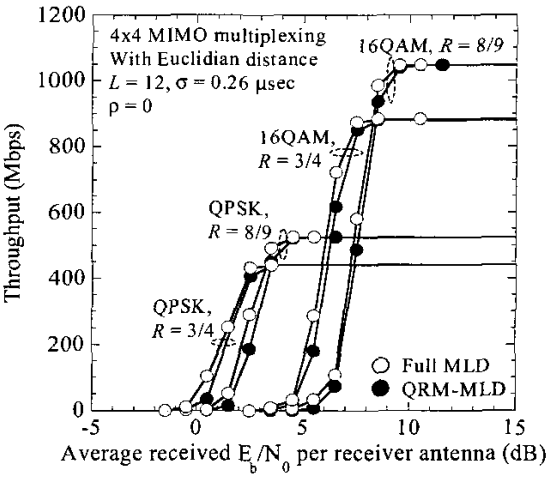

Figure 11. Throughput performance

VI. Conclusion

This paper proposed likelihood function generation of complexity-reduced Maximum Likelihood Detection with QR Decomposition and M-algorithm (QRM-MLD) suitable for soft-decision Turbo decoding and investigated the throughput performance using QRM-MLD with the proposed likelihood function in multipath Rayleigh fading channels for OFCDM MIMO multiplexing. We also presented a QRM-MLD configuration based on channel estimation and ranking of transmitted signals applying a time-multiplexed orthogonal pilot channel. Simulation results showed that by using the proposed likelihood function generation for soft-decision Turbo decoding following QRM-MLD in 4-by-4 MIMO multiplexing, the required average received E_b/N_0 at the average BLER of 10^{-2} at a 1-Gbps data rate was reduced significantly compared to that using hard-decision decoding in OFCDM access with 16 QAM modulation, the coding rate of 8/9, and 8-code multiplexing for the spreading factor of 8 assuming a 100-MHz bandwidth. Furthermore, it was shown that by employing QRM-MLD associated with soft-decision Turbo decoding for 4-by-4 MIMO multiplexing, the throughput values of 500 Mbps and 1 Gbps are achieved at the average received E_b/N_0 of approximately 4.0 and 8.8 dB by QPSK with the coding rate of $R = 8/9$ and 16QAM with $R = 8/9$, respectively, for OFCDM access assuming a 100-MHz bandwidth in a six-path Rayleigh fading channels.

References

[1] N. Yee, J.-P. Linnartz, and G. Fettweis, "Multi-Carrier CDMA in indoor wireless radio networks," PIMRC'93, pp. 109-113, Sept. 1993.

[2] K. Fazel and L. Papke, "On the performance of convolutional-coded CDMA/OFDM for mobile communication systems," PIMRC'93, pp. 468-472, Sept. 1993.

[3] G. Fettweits, A.S. Bahai, and K. Anvari, "On multi-carrier code division multiple access (MC-CDMA) modem design," IEEE VTC'94, pp. 1670-1674, June 1994.

[4] H. Atarashi, S. Abeta, and M. Sawahashi, "Broadband packet wireless access appropriate for high-speed and high-capacity throughput," IEEE VTC2001-Spring, pp. 566-570, May 2001.

[5] H. Atarashi, S. Abeta, and M. Sawahashi, "Variable spreading factor orthogonal frequency and code division multiplexing (VSF-OFCDM) for broadband packet wireless access," IEICE Trans. Commun., vol. E86-B, no. 1, pp. 291-299, Jan. 2003.

[6] N. Maeda, Y. Kishiyama, H. Atarashi, and M. Sawahashi, "Variable spreading factor-OFCDM with two dimensional spreading that prioritizes time domain spreading for forward link broadband wireless access," IEEE VTC2003-Spring, pp. 127-132, Apr. 2003.

[7] G.J. Foschini, Jr., "Layered space-time architecture for wireless communication in a fading environment when using multi-element antennas," Bell Labs Tech. J., pp. 41-59, Autumn 1996.

[8] R.D. Murch and K.B. Letaief, "Antenna Systems for Broadband Wireless Access," IEEE Commun. Mag., vol. 40, no. 4, pp. 76-83, April 2002.

[9] P. W. Wolniansky, G. J. Foschini, G. D. Golden, and R. A. Valenzuela, "V-BLAST: an architecture for realizing very high data rates over the rich-scattering wireless channel," in Proc. 1998 URSI International Symposium on Signals, Systems, and Electronics, pp. 295-300, Sep. 1998.

[10] A. van Zelst, R. van Nee, and G.A. Awater, "Space division multiplexing (SDM) for OFDM systems," IEEE VTC2000-Spring, pp. 1070-1074, May 2000.

[11] K.J. Kim and J. Yue, "Joint channel estimation and data detection algorithms for MIMO-OFDM systems," in Proc. Thirty-Sixth Asilomar Conference on Signals, Systems and Computers, pp. 1857-1861, Nov. 2002.

[12] H. Kawai, K. Higuchi, N. Maeda, and M. Sawahashi, "Performance of QRM-MLD employing two-dimensional multi-slot and carrier-averaging channel estimation using orthogonal pilot channel for OFCDM MIMO multiplexing in multipath fading channel," in Proc. Wireless 2004.